American Mineralogist, Volume 73, pages 77–90, 1988

Experimental investigation of the smectite to illite reaction: Dual reaction mechanisms and oxygen-isotope systematics

GENE WHITNEY, H. ROY NORTHROP*
U.S. Geological Survey, M.S. 904, Box 25046, Denver, Colorado 80225, U.S.A.

ABSTRACT

K-saturated <2-μm and <0.1-μm fractions of Wyoming bentonite (SWY-1) and two other smectite starting materials were treated hydrothermally at 250 to 450 °C for times up to 220 d with a 1:1 mass ratio of solid to distilled water. Progress of the illitization reaction was monitored mineralogically and isotopically. In all experiments, the expandability of the interstratified illite/smectite (I/S) decreased rapidly at first and then asymptotically approached a constant value at long run times (220 d). I/S stabilized at an expandability of 45% at 250 °C, 38% at 300 °C, 22% at 350 °C, 12% at 400 °C, and 4% at 450 °C for the <2-μm fraction. The <0.1-μm fraction reacted more rapidly to a stable expandability, but the final expandability was higher than that of the <2-μm fraction at the same temperature. Saturating the I/S run products with Na expanded many of the collapsed layers and randomized interstratification. This behavior indicates that many of the 10-Å layers were not illite because interlayer K was not fixed. Thus, K-dominated experimental systems may give reaction rates that are unrealistically high for most natural systems because the "illite" layers measured initially are not truly illite.

The $\delta^{18}O$ compositions of the experimental fluids and solids parallel the expandability curves. At each temperature the $\delta^{18}O$ values shifted rapidly from that of the starting fluid (−19.6‰) and starting solids [+19.2‰ for SWY-1 (<2 μm)] and then approached constant values with increasing run time. Both the mineralogy and the pathway of oxygen-isotope resetting as a function of illitization demonstrate that the illitization reaction proceeded in three stages via two reaction mechanisms. During the first (random) stage, a transformation reaction mechanism dominated, forming only random I/S, and approximately 65% of the oxygen in each layer was reset when illitized. The second stage of the reaction was a transition stage, during which random and ordered I/S coexisted as separate phases. In the third (ordered) stage of the reaction, a neoformation reaction mechanism dominated, producing only ordered I/S. During the ordered stage of the reaction, the degree of isotopic resetting was directly proportional to the degree of illitization: illite layers were 100% reset isotopically as they formed. These data show that the illitization reaction, at least for the materials and the temperature and pressure conditions used in these experiments, is more complex than previously believed and is neither a simple transformation nor neoformation process, but is a combination of the two.

INTRODUCTION

Interstratified illite/smectite (I/S) is common in many geologic environments. I/S is an important petrologic indicator even though its reactivity and stability are poorly understood. The expandability of I/S (percent expanding layers in the interstratified phase) has been used as a temperature indicator or thermal maturation indicator. Although maximum temperatures have been deduced for rocks from expandability measurements, it is not uncommon to find "anomalous" expandabilities in rocks of known thermal history. An inverse relationship between temperature and expandability cannot be applied precisely because quantitative effects of key parameters are not known. Experimental work by Eberl and Hower (1976), Roberson and Lahann (1981), Howard and Roy (1985), Inoue (1983), and others has demonstrated qualitatively or semiquantitatively that temperature, time, fluid composition, and solid composition influence the course and rate of the reaction. However, it is not currently possible to predict the extent of illitization, even if all of the above variables are known, because of a lack of systematic experiments.

This paper reports the first of a series of investigations designed to study the effects of several variables on the rate and extent of illite formation from smectite. These investigations start with a relatively simple system consisting of natural smectite with all cation-exchange sites occupied by K. The extent of reaction was measured by

* Deceased.

0003–004X/88/0102–0077$02.00

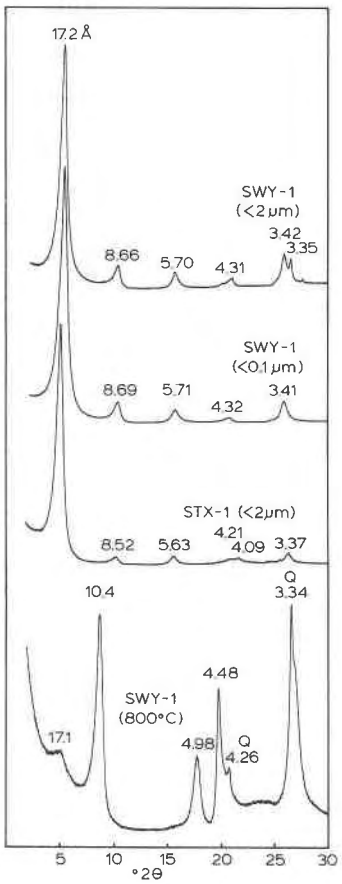

Fig. 1. X-ray diffraction patterns of starting materials. Materials have been saturated with K and then saturated with Na. All samples are oriented and saturated with ethylene glycol and were X-rayed with Cu$K\alpha$ radiation. The d spacings are shown in ångströms.

X-ray diffraction and isotopically in order to provide information about the rate and mechanism of the reaction.

Materials and methods

Starting materials

The primary starting material was the <2-μm fraction of SWY-1 (Wyoming bentonite) from the Source Clay Minerals Repository collection. Parallel experiments were performed using the <0.1-μm fraction of SWY-1, the <2-μm fraction of STX-1 (Texas bentonite), and the <2-μm fraction of SWY-1 that had been heated in air to 800 °C for 1 h. SWY-1 contains quartz in the <2-μm fraction, but the <0.1-μm fraction is pure smectite. STX-1 contains small amounts of cristobalite and a zeolite. SWY-1 (<2 μm) exhibits a glycol thickness of 17.14 Å, and SWY-1 (<0.1 μm) and STX-1 have glycol thicknesses of 16.9 Å. Chemical analyses and cation ratios for these materials are listed in Table 1. X-ray diffraction patterns for starting materials are shown in Figure 1. Starting materials were size-separated while in the Na-saturated state, then saturated with K. All were saturated with K by stirring in 1N KCl overnight, followed by washing until the supernatant was chloride free.

Table 1. Chemical compositions and cation ratios for starting materials

	SWY-1 (<2 μm)	SWY-1 (<0.1 μm)	SWY-1 (800 °C)	STX-1 (<2 μm)
SiO_2	63.7	60.1	65.4	64.8
Al_2O_3	18.9	21.3	21.5	18.9
Fe_2O_3*	3.90	4.41	4.45	0.68
MgO	2.31	2.75	2.68	2.90
CaO	0.09	0.05	0.06	0.06
Na_2O	0.22	0.15	0.21	0.15
K_2O	3.54	3.66	3.98	3.64
TiO_2	0.09	0.08	0.09	0.22
LOI	6.77	7.53	1.99	8.57
Total	99.52	100.03	100.36	99.92
Cation ratios for starting materials based on $O_{10}(OH)_2$				
Si	4.00**	3.90	4.00**	4.00**
Al	1.54	1.62	1.54	1.63
Fe	0.20	0.23	0.20	0.04
Mg	0.24	0.27	0.24	0.32
Ca	0.01	0.00	0.01	0.00
K	0.31	0.30	0.31	0.34
Na	0.03	0.02	0.02	0.02

* Total Fe as Fe_2O_3.
** Some SiO_2 subtracted out as a discrete silica phase to reduce tetrahedral occupancy to 4.00.

Experimental design and techniques

The purpose of the experiments was to measure the rate of illitization by measuring the change in the expandability of I/S as a function of temperature and time, and to determine the pathway, or mechanism, of the reaction. Each starting material was run at 250, 300, 350, 400, and 450 °C for times of 1, 7, 14, 30, 60, 120, and 220 d (with a few exceptions). For each run, 60 mg of air-dried clay was weighed into a Au capsule with 60 μL of distilled water. Each capsule was arc-welded shut and weighed before and after hydrothermal treatment to detect leaks. Capsules were placed in calibrated cold-seal reaction vessels that were horizontally oriented in tube furnaces. Temperatures were maintained to within 2 °C of the desired temperatures with proportional controllers. Temperatures were continuously monitored and recorded with a data logger-recorder. All experiments were run at 100 MPa (1 kbar) pressure, with water as the pressure medium.

Analytical techniques

Each Au capsule was opened under vacuum, and the water was extracted for oxygen-isotope analysis using a device specially designed and built for that purpose. A portion of the solids from many of the runs was also analyzed isotopically, using the technique of Clayton and Mayeda (1963), in which oxygen is liberated with BrF_5 and converted to CO_2 and measured on a Finigan MAT 250 mass spectrometer. Oxygen-isotope measurements on the fluids and solids are reported relative to SMOW and are accurate to within ±0.2‰.

Solids were recovered from the Au capsules, disaggregated gently in a small amount of distilled water with a mortar and pestle, and pipetted onto glass slides to make oriented mounts. Each sample was X-rayed using an automated Siemens D500 diffractometer after being air-dried and after saturation with ethylene glycol. The expandability of each sample was determined by comparing with calculated diffraction patterns produced with the algorithm of Reynolds (1980) and using the techniques of Środoń (1980, 1984). Expandabilities reported are within ±5%.

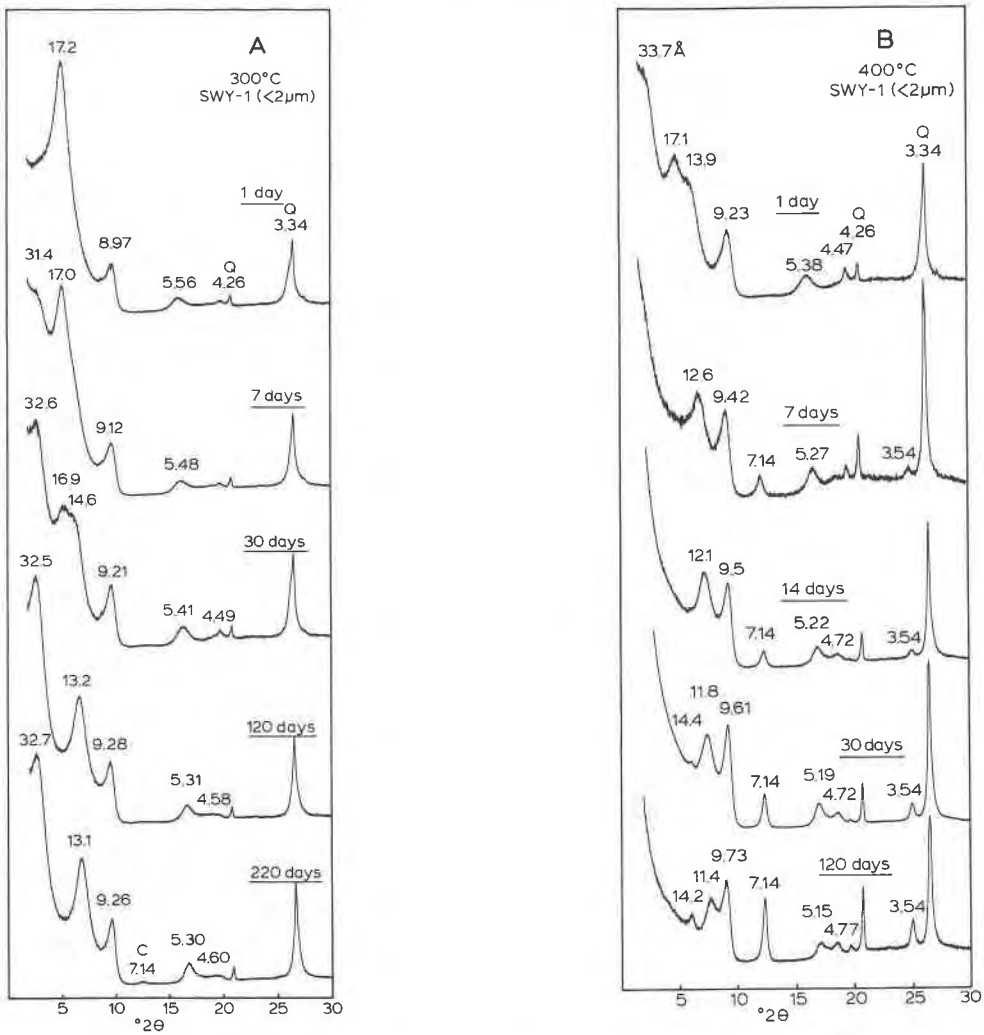

Fig. 2. X-ray diffraction patterns for run products from the (a) 300 °C series and (b) 400 °C series showing the reduction in expandability and the change from random to ordered interstratification with increasing run time. All samples are oriented and saturated with ethylene glycol. The *d* spacings are shown in ångströms.

Many of the run products were Na-saturated in order to determine the proportion of nonexpandable layers. This test was performed because K-saturated smectites sometimes exhibit collapsed layers that expand when exposed to a different interlayer cation. The measurement of nonexpandable layers gives a more complete picture of the nature of the reaction than simply measuring the apparent proportion of illite layers in K-saturated interstratified I/S.

Mineralogical results

Reaction trends

The dominant run product in all experiments was interstratified illite/smectite. Other phases produced include chlorite, kaolinite, quartz, and cristobalite. These byproducts generally are minor, but the chlorite comprised a significant proportion of run products at 400 and 450 °C.

Expandabilities of the run products were monitored carefully because expandability was the main measure of reaction progress. Expandabilities are compiled for SWY-1 (<2 μm) in Table 2. Initial examination of the run products, which were saturated with K, shows that the expandability decreased systematically with increasing temperature and run time. For example, Figure 2 shows X-ray diffraction data for runs of increasing time at 300 and 400 °C. The systematic decrease in expandability can be seen in the migration of the peaks near 9–10° and 16–17° 2θ (Reynolds, 1980). Distinguishing randomly interstratified I/S from ordered I/S at expandabilities greater than 70% is difficult, but the appearance of peaks near 2θ values of 3° and 6–8° signal the appearance of R1-ordered I/S at lower expandabilities. Importantly, some samples contain a mixture of randomly interstratified and R1-ordered I/S, as evidenced by the existence of the ordering

TABLE 2. Mineralogical and isotopic data for SWY-1 (<2 μm) run products

Sample	Temp. (°C)	Time (d)	Exp.* (K)	Ord. type**	Exp.† (Na)	$\delta^{18}O$ (fluid)	$\delta^{18}O$ (solid)	Other phases‡
SWY-1§	—	0	100	—	100	−19.7	+19.2	Q, M
A132	250	7	83	R	92	−17.4	+14.9	Q
A133	250	14	78	R	91	−16.7	+13.9	Q, M
A134	250	30	57	R	91	−15.8	+13.5	Q, M
A135	250	60	52	R	90	—	+12.2	Q, M
A136	250	120	45	R + O	90	−14.9	+11.0	Q
A137	250	220	44	R + O	89	−14.9	+9.6	Q
A141	300	1	70	R	92	−16.6	+13.7	Q, M
A142	300	7	58	R + O	91	−14.4	+9.8	Q, M
A143	300	14	50	O + R	90	—	+8.7	Q, M
A144	300	30	45	O + R	90	—	+7.5	Q, M
A146	300	120	35	O	82	−12.1	+5.3	Q
A147	300	220	35	O	78	−11.4	+4.2	Q, C
A151	350	1	47	O + R	90	−13.6	+8.1	Q, M
A152	350	7	41	O + R	89	—	+6.0	Q, M
A153	350	14	34	O	88	−12.1	+5.0	Q
A154	350	30	27	O	87	—	+4.0	Q, C
A155	350	60	24	O	80	—	+1.8	Q, C
A156	350	120	21	O	76	−9.9	+1.4	Q, C
A161	400	1	45	O + R	90	—	—	Q, M
A162	400	7	28	O	84	—	—	Q, C
A163	400	14	23	O	81	−9.1	+0.6	Q, C
A164	400	30	14	O	68	—	—	Q, C
A166	400	120	12	O	64	—	—	Q, C
A171	450	1	23	O + R	89	—	—	Q, C
A172	450	7	12	O	84	—	—	Q, C
A173	450	14	8	O	8	—	—	Q, C
A174	450	30	5	O	5	—	—	Q, C
A175	450	60	4	O	4	−6.8	—	Q, C
A176	450	120	4	O	4	—	—	Q, C

* Expandability (in percent) for samples as initially mounted (K-saturated).

** Ordering type: R = random interstratification, O = ordered interstratification. When both random and ordered I/S are present, the predominant type is listed first.

† Expandability (in percent) for samples after saturation with Na.

‡ Q = quartz, M = mica, C = chlorite. The starting material for SWY-1 (<2 μm) contained discrete quartz and a trace of mica (sometimes not detectable in run products).

§ Starting material.

peaks described above, with the persistence of the most intense I/S peak associated with random interstratification at 5.2° 2θ (e.g., 7-d run time in Fig. 2a and 1-d run time in Fig. 2b). Because both randomly interstratified and ordered I/S exhibit the peaks near 9–10° and 16–17° 2θ, and because no exceptional broadening of those peaks or doublets are apparent, the coexisting randomly interstratified and ordered I/S must have approximately the same expandabilities. The R1-ordered I/S first appeared when the randomly interstratified I/S had reached approximately 60% expandable, and when the I/S had reached 40% expandable, the randomly interstratified phase had completely disappeared and only R1-ordered I/S remained.

The overall trends in expandability for the initial run products of the <2-μm fraction of SWY-1 as a function of temperature and time are shown in Figure 3a. At each temperature, the expandability dropped rapidly at first and then asymptotically approached some constant value at longer run times. The final expandability was different for each temperature and ranged from approximately 50% at 250 °C to <5% at 450 °C. The shortest runs at 250 °C seem to form a trend that is unlike the other curves and unlike the trend for the longer runs at 250 °C. This portion of the curve represents run products that are strictly randomly interstratified and may suggest that the randomly interstratified I/S followed a different reaction trend than the ordered I/S.

The other starting materials give products that show similar trends, although the final expandability differs for different materials and the time required to reach the final expandability is different for some starting materials (Table 3). Figure 3b shows the expandability vs. time plot for the <0.1-μm fraction of SWY-1. The final expandability at each temperature is higher than that of the coarser fraction (Fig. 3a), but the time required to reach that expandability was less. The I/S had essentially stopped reacting after only 14 d, whereas the <2-μm fraction continued to react for at least 100 d. The STX-1 and SWY-1 (800 °C) produced reaction curves with similar shapes. The heated SWY-1 (800 °C) exhibited reaction rates similar to the unheated SWY-1, but final expandabilities were higher (Fig. 3c). The STX-1 material is very similar chemically to SWY-1 (<2 μm), and the final expandabilities and reaction rates were approximately the same (Fig. 3d).

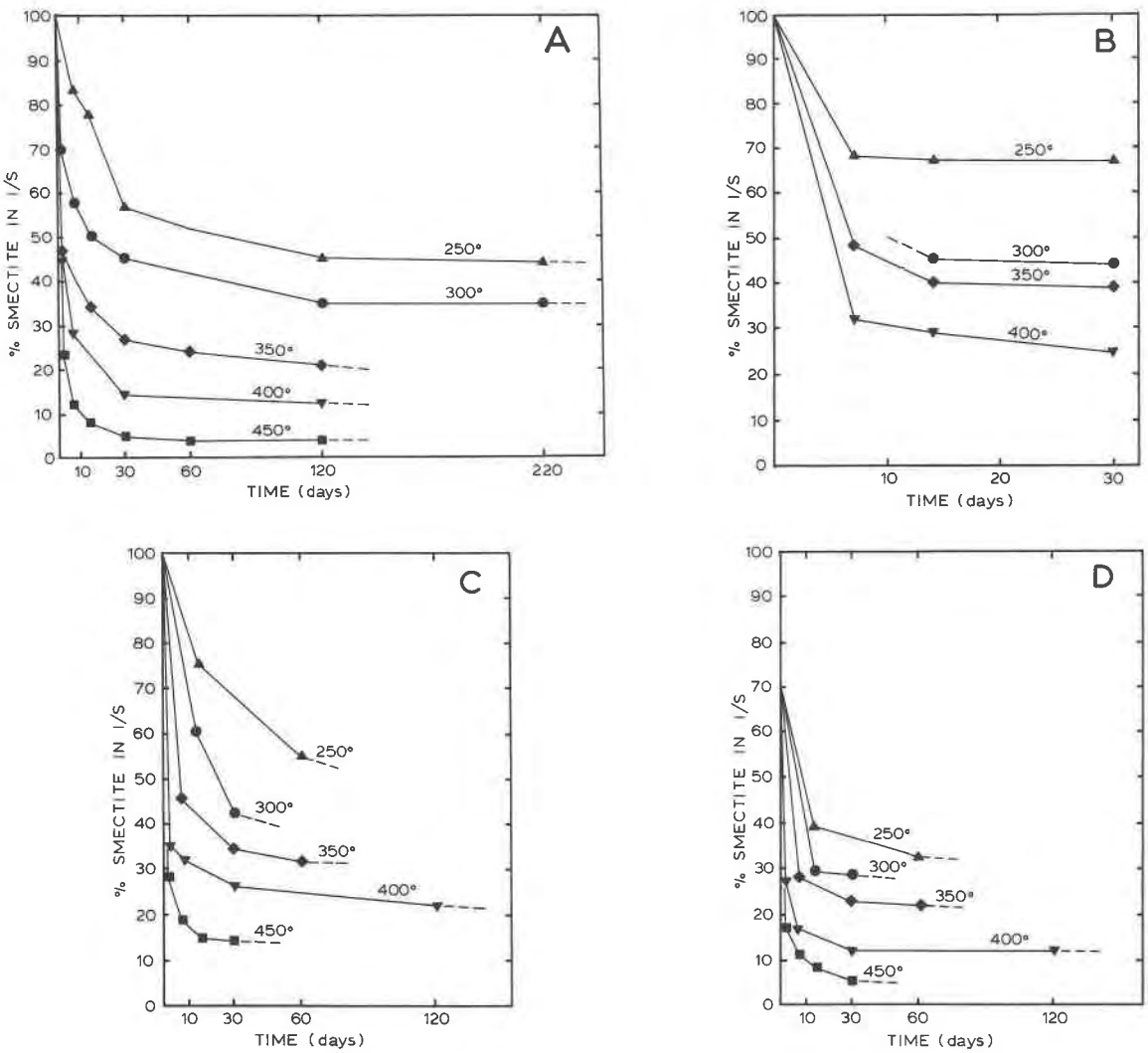

Fig. 3. Expandability of the run products as a function of time at each temperature for the different smectite starting materials: (a) SWY-1 (<2 μm), (b) SWY-1 (<0.1 μm), (c) SWY-1 (800 °C), (d) STX-1. Note that the final expandability is inversely related to temperature.

The differences in reactivity among the smectite starting materials at 400 °C are shown in Figure 4. The starting materials are quite similar chemically (see Table 1). Some key differences are that STX-1 is very low in Fe, SWY-1 (<0.1 μm) contains no discrete silica phase, and SWY-1 (800 °C) is largely anhydrous and completely oxidized. All contain virtually the same amount of K, yet the reaction of the materials differed in two ways: the expandability at which the reaction stopped at each temperature and the rate at which each material reacted to that final expandability. Figure 4 shows the expandability trends for each material in the 400 °C experiments. After 1 d, STX-1 was least expandable (27%), SWY-1 (<2 μm) was most expandable (45%), and SWY-1 (800 °C) was intermediate. After 7 d, STX-1 was still least expandable (17%), but SWY-1 (<2 μm) had become less expandable than SWY-1 (800 °C) and SWY-1 (<0.1 μm). SWY-1 (<2 μm) and STX-1 ended with almost exactly the same expandability in the longer runs, but clearly followed different paths to reach that expandability. Likewise, SWY-1 (800 °C) and SWY-1 (<0.1 μm) attained about the same expandability after 30 d but apparently had slightly different reaction rates.

Na-saturation experiments

Run products of SWY-1 (<2 μm) were Na-saturated to determine how many of the collapsed layers were re-expandable and how many were irreversibly collapsed. (In this discussion, the term "collapsed" is used only as a descriptive term and is not intended to imply a mechanism of formation.) The expandabilities of the Na-saturated run products are included in Table 2. A large proportion of the collapsed layers expanded when Na-saturated, except the longest runs at 450 °C. Figure 5

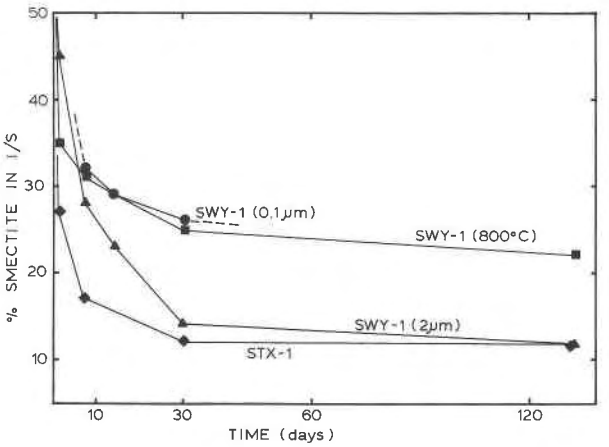

Fig. 4. Expandability of I/S vs. time for the 400 °C series of each smectite starting material. All samples are in their initial K-saturated state. Despite mineralogical and chemical similarities among the starting materials, the rate and extent of reaction vary considerably.

shows X-ray diffraction data of a K-saturated sample as it originally appeared after removal from the capsule and after saturation with Na. For the lower-temperature, shorter experiments, all but about 10% of the collapsed layers re-expanded. At higher temperatures and longer run times, more of the layers remained collapsed after saturation with Na. At 450 °C and long run times, virtually all of the collapsed layers remained collapsed. Figure 6 shows the plot of Na-saturated expandability vs. time for all temperatures, and comparison with Figure 3a confirms that the proportion of layers that is irreversibly collapsed (i.e., "true" illite layers) is much smaller than the original proportion of collapsed layers in the run products.

Additional tests were performed in order to ensure that these data were not simply artifacts. For example, several samples of the K-saturated run products were suspended and washed several times without saturation with Na in order to make sure that this treatment alone would not cause an increase in expandability. Resaturation of Na-saturated run products with K did not cause the layers to collapse again to the original expandability. Thus, saturation with Na caused irreversible expansion of those collapsed layers. However, dehydration and rehydration appear to play some role in the preservation of ordering. Some samples that were completely dehydrated during the oxygen-isotope analysis process exhibited more random I/S component than duplicate samples that had never been completely dehydrated.

Excess K runs

In the majority of the runs, the amount of K in the system was sufficient to satisfy the cation-exchange capacity of the smectite, i.e., about 0.31 equivalents per $O_{10}(OH)_2$. In order to crudely determine the effect of K availability on the illitization reaction, an increment of K was added to several runs in order to make the amount of K in the system approximately equal to 0.6 equivalents per $O_{10}(OH)_2$. The results are listed in Table 4. In some runs, the additional K simply accelerated the reaction, making the run products more illitic. In the higher-temperature, longer runs, however, the additional K had minor effect on the expandability of the I/S produced, but suppressed the amount of accessory minerals produced as byproducts of the reaction. For example, the original runs at 400 and 450 °C produced substantial quantities

TABLE 3. Mineralogical and isotopic data for run products from secondary starting materials

Sample	Temp. (°C)	Time (d)	Expand.* (K)	Ord. type**	$\delta^{18}O$ (fluid)	Other phases†
			SWY-1 (<0.1 μm)			
BA32	250	7	68	R	−18.1	—
BA33	250	14	67	R	−16.8	—
BA34	250	30	67	R	−16.1	—
BA42	300	7	49	R + O	−14.0	—
BA43	300	14	45	O + R	−13.0	—
BA44	300	30	44	O + R	−12.4	—
BA52	350	7	48	R + O	−13.9	—
BA53	350	14	40	O + R	−11.2	—
BA54	350	30	39	O	−11.1	—
BA62	400	7	32	O + R	−10.1	—
BA63	400	14	29	O	−9.6	C
BA64	400	30	25	O	−8.7	C
			STX-1 (<2 μm)			
STX-1‡	—	0	100	—		Cr
A233	250	14	39	O + R		Cr
A235	250	60	33	O		Cr
A243	300	14	29	O		Cr
A244	300	30	29	O		Cr, Q
A252	350	7	28	O		Cr
A254	350	30	23	O		Cr
A255	350	60	22	O		Cr, Q
A261	400	1	27	O		Cr
A262	400	7	17	O		Cr, Q
A264	400	30	12	O		Cr, Q
A266	400	120	12	O		Cr, Q, C
A271	450	1	17	O		Cr
A272	450	7	11	O		Cr, Q
A273	450	14	8	O		Cr, Q, C
A274	450	30	5	O		Cr, Q, C
			SWY-1 (800 °C)			
SWY-1‡	—	0	0	—		Q
A833	250	14	75	R		Q
A835	250	60	55	R		Q
A843	300	14	60	R		Q
A844	300	30	42	R		Q
A852	350	7	25	R + O		Q
A854	350	30	25	O + R		Q
A855	350	60	23	O		Q, Cr
A861	400	1	35	O + R		Q
A862	400	7	31	O		Q, Cr
A864	400	30	25	O		Q
A866	400	120	22	O		Q, C
A871	450	1	28	O		Q
A872	450	7	18	O		Q, C
A873	450	14	15	O		Q, C
A874	450	30	14	O		Q, C

* Expandability in percent for original run products.

** Ordering type: R = random interstratification, O = ordered interstratification. When both types of ordering are present, the dominant type is listed first.

† Cr = cristobalite, Q = quartz, C = chlorite.

‡ Starting material.

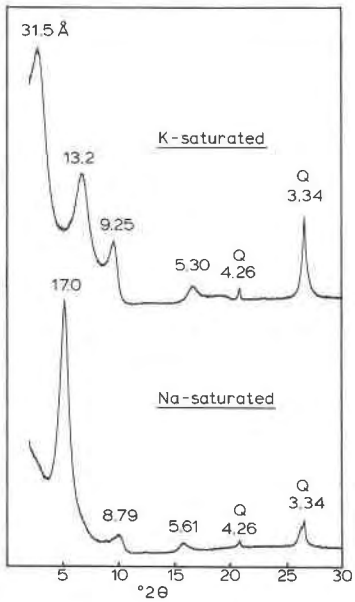

Fig. 5. X-ray diffraction patterns for sample A156 as initially mounted (K-saturated, top) and after saturation with Na. The ordered I/S becomes largely randomized and expandability increases markedly when saturated with Na.

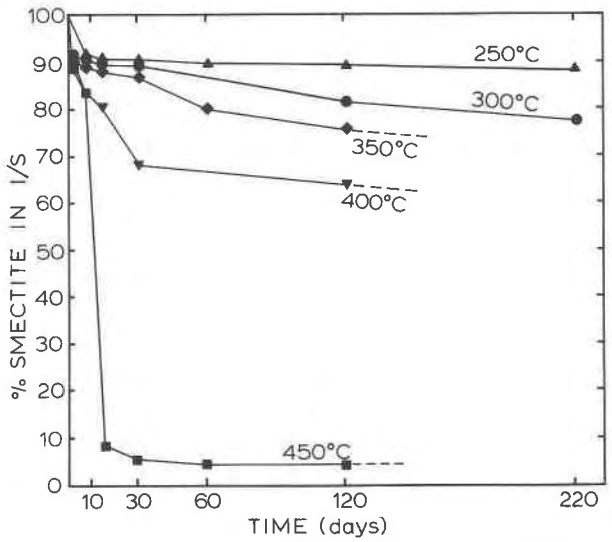

Fig. 6. Expandability of I/S vs. time at each temperature for the run products after saturation with Na.

of chlorite as a byproduct (Fig. 7). When additional K was added to the system, no chlorite was produced, and the I/S was only slightly more illitic than in the low-K runs.

Oxygen-isotope results

In addition to the expandabilities of the I/S, the oxygen-isotope compositions of both the fluids and solids were monitored to provide another measure of reaction progress (Tables 2 and 3). Oxygen mass balance in the experimental system was checked by calculation of fluid and solid contributions. Fluid and solid compositions, which initially differed by 38.9‰, began to converge as illitization progressed (Fig. 8a). Because oxygen constitutes the structural skeleton of the reacting minerals, the degree of isotopic resetting is an indication of the extent of rearrangement of the mineral structure. The oxygen-isotope compositions of the fluids and solids from the SWY-1 (<2 μm) are shown in Figure 8a as a function of time for each temperature. The isotopic trends are similar to the expandability trends: the $\delta^{18}O$ values of both the solids and the fluids changed rapidly at first but approached a constant value at longer run times. The extent of isotopic compositional change was greater at higher temperatures. Analysis of the fluid isotopic compositions from the reactions of the finer fraction of SWY-1 (<0.1 μm) shows a similar trend (Fig. 8b).

Discussion

Nature of the illitization reaction

There is some debate about whether the illitization reaction proceeds via a layer-by-layer transformation or dissolution-precipitation mechanism (Nadeau et al., 1984a, 1984b, 1984c, 1985a, 1985b; Nadeau and Bain, 1986; Bethke and Altaner, 1986; Sawhney and Reynolds, 1985). The energy requirements of the two mechanisms may be quite different because transformation could require the breaking of only a few structural bonds in order to build a layer charge on the 2:1 layer, whereas neoformation (dissolution followed by precipitation) requires profound breakdown and reassembly of the structure. The experimental data indicate that the illitization of K-saturated bentonitic smectite proceeds via two separate mechanisms and that the reaction can be divided into three distinct stages.

Isotopic evidence for dual reaction mechanisms

The relationship between the change in oxygen-isotope composition and the extent of illitization is shown in Fig-

Table 4. Expandability of run products from excess K experiments

Sample	Temp. (°C)	Time (d)	Expand.* (K)	Ord. type**	Other phases†
CK134	250	30	55	R + O	Q, M
CK135	250	60	42	O + R	Q, M
CK144	300	30	33	O + R	Q, M
CK145	300	60	33	O + R	Q, M
CK154	350	30	24	O	Q, M
CK155	350	60	20	O	Q, M
CK164	400	30	11	O	Q, M
CK165	400	60	10	O	Q, M
CK174	450	30	3	O	Q, M
CK175	450	60	2	O	Q, M

* Expandability in percent for original run products.

** Ordering type: R = random interstratification, O = ordered interstratification. When both types of ordering are present, the dominant type is listed first.

† Q = quartz, M = mica. Quartz and mica (in trace amounts) are present in starting materials.

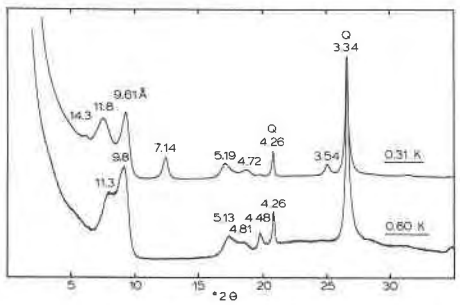

Fig. 7. Comparison of X-ray diffraction patterns of (upper curve) a run containing 0.3 equivalents of K per formula unit of smectite and (lower curve) a run containing 0.6 equivalents of K. The excess K produces more I/S that is more illitic and inhibits the formation of chlorite as a byproduct.

ure 9, where the $\delta^{18}O$ values are plotted vs. expandability. The data in Figure 9 represent isotope and expandability values for several temperatures. Technically, we should be able to draw a pair of lines (one for fluids, one for solids) for each experimental temperature, but our data do not provide sufficient resolution for such a separation. The data fall along two closely constrained sets of lines. One set represents samples dominated by random interstratification, and the other set represents samples dominated by ordered interstratification. These data suggest that two different reaction mechanisms produced the two different types of interstratification.

The extent of isotope equilibration for each increment of the reaction may be estimated by using the measured difference between solid and fluid isotopic compositions from Figure 8a and comparing them to the starting difference (38.9‰) and the equilibrium difference. The difference at equilibrium is the fractionation factor and is calculated from Savin (1980) for each temperature. Figure 10 shows a family of lines that connect the starting difference with the equilibrium difference for each temperature. Plotting the measured final difference for each temperature on these lines gives a measure of equilibration for each temperature. Each step of the reaction may be expressed in terms of the extent of equilibration. Figure 11 shows the extent of equilibration at each temperature as a function of time. This plot clearly shows that the reaction stopped short of isotopic equilibrium at all temperatures for the run times used. The higher-temperature reactions approached isotopic equilibrium more closely than the lower-temperature reactions.

The relationship between the degree of isotopic equilibration and the extent of illitization is shown in Figure 12. Again, two lines indicate different relationships between the extent of illitization and isotopic resetting for random and ordered I/S. The trend of random illitization, when extrapolated to zero expandability (100% illite layers) would only reach about 65% isotope equilibration Therefore the formation of random I/S was accompanied by incomplete isotopic resetting and could be considered a "transformation" reaction because the structure was not completely broken down and reassembled to make illite layers. Even though the entire structure was not reset isotopically, the fact that it was 65% reset for each increment

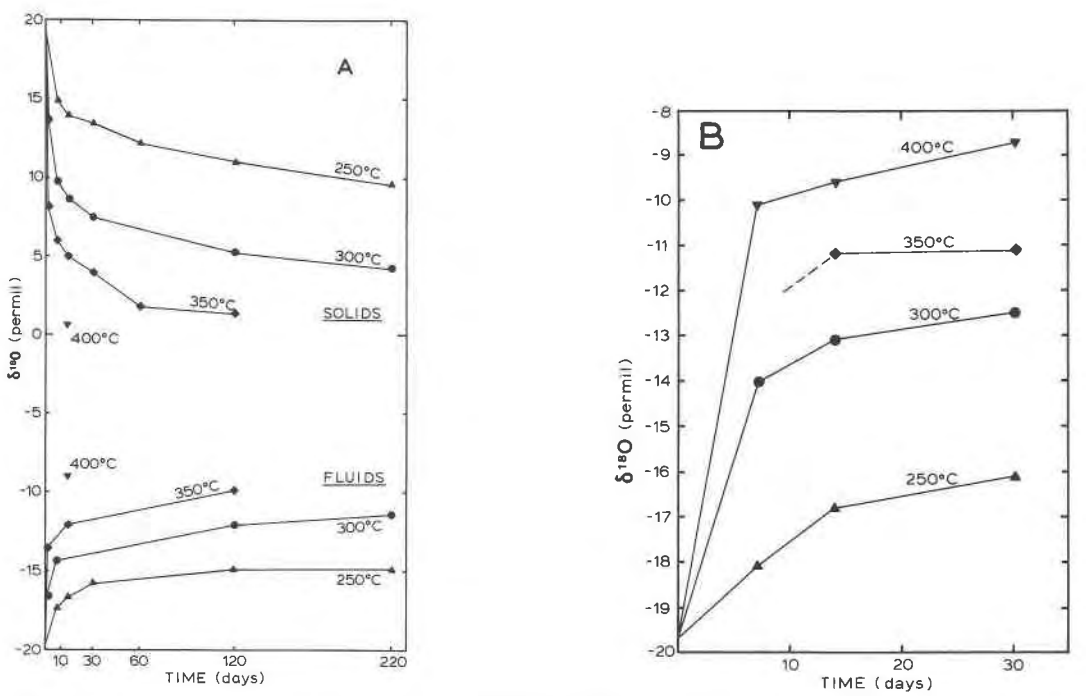

Fig. 8. Oxygen-isotope composition of run products as a function of time at each temperature: (A) fluid and solid compositions of SWY-1 (<2 μm) and (B) fluid compositions for SWY-1 (<0.1 μm). Isotope reaction trends are similar to the expandability curves.

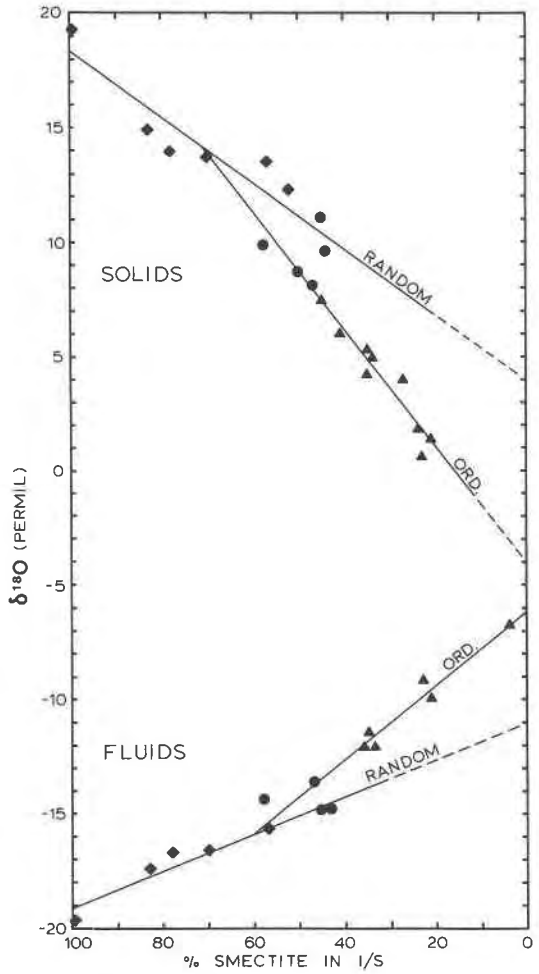

Fig. 9. Oxygen-isotope composition of fluids and solids for SWY-1 (<2 μm) as a function of the expandability of the I/S. The samples dominated by random I/S plot along different lines than the samples dominated by ordered I/S, suggesting different rates of isotopic resetting. Diamonds = random I/S; circles = mixture of random and ordered I/S; triangles = ordered I/S.

of illite layers produced, coupled with the observation that a certain number of illite layers did not re-expand, suggests that even the first (random) stage of the reaction was accompanied by substantial structural rearrangement.

The ordered I/S trend does not begin at 100% expandability but intersects the random I/S line, confirming our observations that the formation of ordered I/S did not start until the random I/S was substantially illitized. Extrapolation of the ordered I/S trend shows that formation of the ordered I/S was accompanied by complete isotopic resetting and therefore could be considered a dissolution-precipitation reaction. What is not known is the textural relationship between the two types: the dissolution-precipitation process may actually have been topotactic replacement, maintaining the original morphological characteristics, or may represent the formation of overgrowths

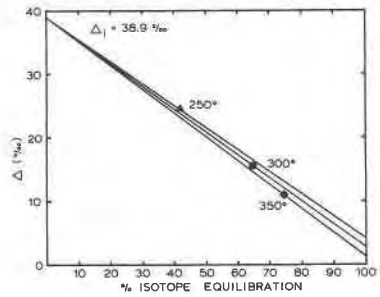

Fig. 10. A plot of the difference in isotope composition between fluids and solids (Δ) as a function of the extent of equilibration. The starting difference is assumed to represent zero percent equilibration. The fractionation factors representing complete equilibration were taken from Savin (1980). The points along the lines represent the "final" differences in composition at each temperature and show how the percent equilibration is measured.

and nucleation and growth of new crystals. Further work is required to determine the exact processes involved.

One puzzling aspect of this conclusion is the fact that the "illite" layers measured and plotted here are not all true illite (irreversibly collapsed) but are largely the re-expandable layers described above. Although the layer charge developed on the "illitized" 2:1 layers must be insufficient to cause irreversible collapse, its development was accompanied by complete isotopic resetting. Thus, the reaction proceeded in the same way whether a small or large layer charge was developed. Thus, the composition of the interlayer cation must set the "endpoint" of the layer charge development. When K is the dominant cation, a low layer charge is produced, perhaps because the layers collapse at a lower value, effectively stopping the reaction. When a cation with a higher hydration en-

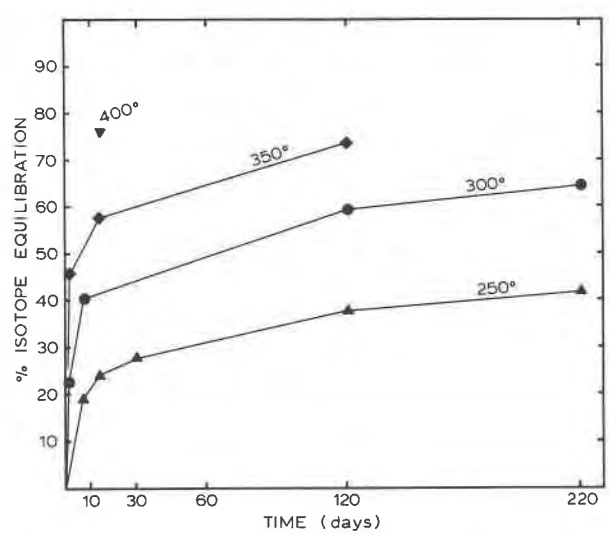

Fig. 11. Percent isotope equilibration vs. time at each temperature. The lines never reach 100%, meaning that the samples do not reach isotopic equilibrium even after 220 d.

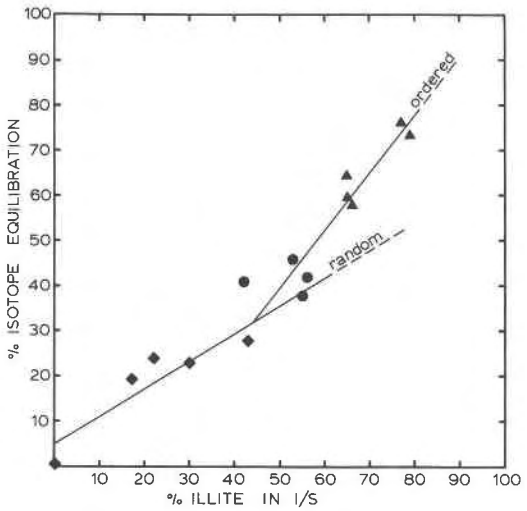

Fig. 12. Percent isotope equilibration vs. percent illite in I/S. Samples dominated by random I/S follow an equilibration path that extrapolates to about 65% equilibration at 100% illite layers. The ordered I/S samples form a line that intersects the random curve and extrapolates to about 100% isotopic equilibration at 100% illite layers. These separate trends suggest that random and ordered I/S form along different reaction paths. Diamonds = random I/S; circles = mixture of random and ordered I/S; triangles = ordered I/S.

ergy is present, the layers are propped open for a longer time, allowing further layer charge to develop prior to collapse around K. Howard and Roy (1985) have demonstrated that layer charge continues to develop in K-deficient solutions. Alternatively, the presence of K in the interlayer region may actually affect the layer charge directly by excluding Al from tetrahedral sites, but this is a question that requires further study.

Mineral evidence for dual reaction mechanisms

Mineral data alone have not provided conclusive evidence in support of a single, universal illitization reaction mechanism (Sawhney and Reynolds, 1985; Nadeau et al., 1985b). The existence of three distinct stages of illitization in these experiments suggests that the illitization reaction is perhaps even more complex than previously thought. If the transition from random I/S to ordered I/S involved a uniform transformation of a single phase at 60 to 80% expandability, then it could be argued that a single reaction mechanism was at work. In fact, this may be the case in some natural I/S. But a 50% expandable, perfectly ordered I/S cannot be formed by transformation of a randomly interstratified precursor. The only way to form perfect R1 ordering in 50% expandable I/S is by direct precipitation, or by illitization of a smectite that has an inherent propensity for ordering. In the present experiments, the initial random I/S decreased in quantity as it increased in proportion of illite layers. The coexistence of both random and ordered I/S in the same samples, exhibiting both characteristic sets of diffraction peaks during the transition stage, strongly suggests that ordered I/S precipitated from solution after the random illitization process had progressed to about 60 to 70% expandability.

If I/S is viewed from the fundamental particle paradigm of Nadeau et al. (1984a, 1984b, 1984c), highly ordered I/S produced in these experiments would require a population of fundamental particles of uniform thicknesses. The ordered stage of the illitization reaction may be interpreted as the growth of uniformly thick fundamental particles that develop more and more illitic layers with increasing temperature and time. The complete isotopic resetting accompanying each new illite layer supports the contention that dissolution and precipitation took place. When saturated with Na, however, these fundamental particles were cleaved because they probably did not have a full mica charge and, once cleaved, could not be reassembled into the original fundamental particles. This would explain the randomization of the Na-saturated I/S, the increase in expandable layers, and the fact that subsequent saturation with K could not reverse the randomization process. The fundamental particles in these experiments were fragile, and once disturbed could not be reassembled.

Observations on illitization reaction rates and kinetics

Eberl and Hower (1976) explored the kinetics of illitization experimentally using amorphous K-bearing starting materials. Their data were described by first-order (or pseudo–first-order) reaction kinetics with respect to smectite layers. Additional experiments by Roberson and Lahann (1981) and Howard and Roy (1985) showed that cation compositions of the fluid also play a major role in the degree of illitization in time-temperature experiments, but they also viewed the illitization reaction as first-order with respect to smectite layers. On the other hand, Pytte (1982) concluded that the reaction he observed in a natural contact metamorphic environment was third-, fourth-, or fifth-order with respect to smectite layers in I/S. Eberl et al. (1978) showed experimentally that the composition of the starting smectite played an important role in reaction rate, and this effect has been confirmed in nature by Chang et al. (1986) and Anjos (1986).

A detailed kinetic analysis of the reaction was not undertaken here. Such a study must ultimately include a systematic variation in fluid composition, temperature, and time. Some observations can be made, however, concerning the reaction progress and rate as a function of temperature and time. Figure 13a shows a first-order kinetics plot of the reaction with respect to smectite layers in the I/S. If the reaction were first-order, the lines would be straight and pass through the origin. A similar plot (not shown) demonstrates that the reaction also was not second-order with respect to smectite layers. Higher-order reaction kinetics become very difficult to interpret and explain with these limited experiments.

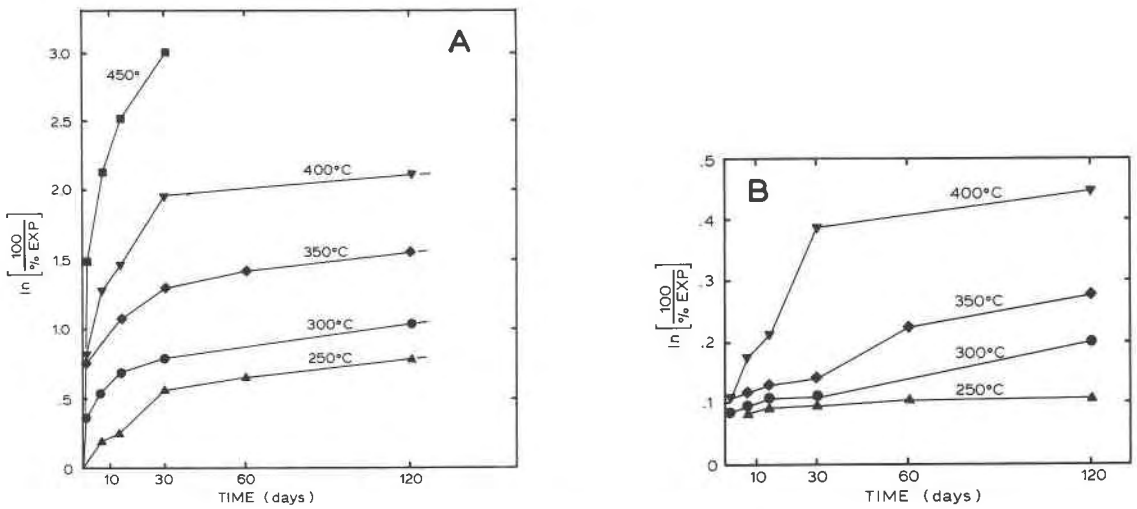

Fig. 13. First-order kinetics plots for (A) the original run products and (B) the Na-saturated run products of SWY-1 (<2 μm). If the reaction were first-order with respect to smectite layers, the lines would be straight.

Because the Na-saturation experiments indicated that there is some question about what constitutes a smectite layer and an illite layer in these run products, the Na-expanded data was also plotted as a first-order kinetics reaction (Fig. 13b). The reaction also was not first-order when viewed from this perspective. It is interesting to note, however, that an inflection occurs in the curves where the run products changed from predominantly random I/S to predominantly ordered I/S.

The different starting materials exhibited different rates of reaction and different final expandabilities even though they are chemically and mineralogically similar. These semiquantitative comparisons do not permit us to predict reaction paths in nature, but do indicate that even closely similar smectite starting materials may follow significantly different reaction paths, depending on such things as particle-size distribution, particle morphology, Fe content and oxidation state, or other factors. The precise quantitative effects of these variables will require further study.

Effects of K availability on the reaction

One of the notable characteristics of these reactions is the fact that the expandability leveled off at long run times at each temperature, regardless of starting material. The fact that the reaction slowed and virtually stopped is partly a result of chemical composition. When excess K was added to the experimental runs, the reaction changed, not just in the number of illite layers in the I/S produced, but in the amount of I/S produced and also in the amount of accessory minerals produced as byproducts of the reaction. For example, the reaction of sample A164 (Fig. 7) can be written as follows:

$$\text{K-exchanged smectite} \xrightarrow{400\ ^\circ\text{C}} \text{I/S} + \text{chlorite} + \text{quartz}.$$

The amount of aluminous chlorite produced is perhaps half the amount of I/S produced, indicating that a significant portion of the original smectite must have been destroyed. The amount of illite produced in I/S was limited by K availability.

For the same material run under the same conditions with additional K added, the reaction changed significantly. Sample CK164 (Fig. 7) contains only I/S and quartz. The reaction may be summarized as follows:

$$\text{K-exchanged smectite} + \text{K}^+ \xrightarrow{400\ ^\circ\text{C}} \text{I/S} + \text{quartz}.$$

Thus, when K was available, the illitization reaction not only produced more illitic I/S, but must have produced more I/S. When K was deficient, some of the original smectite was consumed as the available K was concentrated in the illite layers formed. Byproducts of the destroyed smectite went to make chlorite and quartz.

The fact that the illitization reaction stopped at different expandabilities at different temperatures may be related to the ability of the system to break down existing K-bearing layers to form new illite layers. At the higher temperatures, not only was the I/S more illitic, but more of the layers were irreversibly collapsed (demonstrated by saturation with Na).

Interpretation of natural I/S data

A dual reaction mechanism is consistent with a variety of mineral, chemical, isotopic, and textural data from natural samples of I/S. For example, Bethke et al. (1986) compiled expandability data for 142 samples of I/S from shales, altered bentonites, and hydrothermally altered volcanic rocks. Although their compilation does not include all occurrences of I/S, it represents a significant number of samples from three of the major rock types in

which I/S has been commonly described. In their data, all highly expandable I/S is randomly interstratified, and all highly illitic I/S is ordered. Between the two extremes is a zone (55–70% illite layers) in which both random and ordered I/S may occur. The specific pathway along which the I/S becomes illitized varies for different materials and environments, and the expandability at which the ordered I/S begins to predominate also varies. In fact, these data show that the mode of origin and the starting material may play a major role in the course of the illitization reaction. However, in each case the formation of randomly interstratified I/S could be interpreted to be a transformation reaction, whereas the formation of ordered I/S can be interpreted as a neoformation process.

Środoń et al. (1986) carefully examined the chemistry and layer-charge relationships in I/S and illite from bentonites. One of their conclusions was that the illite layers in I/S do not bear a single uniform layer charge throughout the illitization series (reflected in the amount of fixed K present), but rather exhibit two separate layer charges. At higher expandabilities (>50%), each illite layer carries a charge of about 0.55 equivalents per $O_{10}(OH)_2$, whereas at expandabilities below 50%, each illite layer carries a charge of 1.0 equivalent. These two distinct types of illite layers may correspond to illite formed by transformation during the random stage of illitization (low-charge) and illite formed by neoformation during the ordered stage of the reaction (high-charge). In addition, they noticed that a few percent of the layers in some smectites could be illitized easily by wetting and drying in the presence of K. These layers may have a higher layer charge initially than the rest of the layers in the smectite. These high-charge layers may explain why, in our experiments, even mild hydrothermal treatment collapsed about 10% of the layers that could not be re-expanded by saturation with Na.

Chemically, the composition of the bulk system and the composition of the I/S itself provide additional information about the nature of the illitization reaction. The illitization process described by Hower et al. (1976) probably is limited by K availability of the bulk system, as is the alteration of the bentonite described by Altaner et al. (1984). These data correspond to our observations that the illitization reaction stops when K becomes depleted, even if the temperature is still sufficiently high to drive the reaction. Nadeau and Bain (1986) have observed that, in addition to increased tetrahedral Al, the octahedral cation composition (Al, Mg, Fe) is different for smectite and diagenetic I/S. The I/S samples analyzed were all greater than 70% illite, and the differences in octahedral cation composition suggest that a profound structural rearrangement is required to change the composition of the octahedral sheet. Simple Al-for-Si substitution in the tetrahedral sheet would not alter the octahedral composition. Further work on the octahedral occupancy of I/S with higher expandabilities may help define the transition stage between the random and ordered stages of the reaction.

Keller et al. (1986) observed that, regardless of starting materials, the degree of textural change for several natural samples of I/S is greatest in the illitization interval near 60–70% illite layers. Whitney and Northrop (1987) and Pollastro (1985) have made similar observations on diagenetic I/S in sandstones. This interval corresponds to the range of expandabilities where only ordered I/S was produced and isotopic resetting was complete for each increment of illite formed in our experiments. The change in texture shows that minimal structural change takes place at higher expandabilities (during the random stage of illitization), whereas the morphological changes at lower expandabilities strongly indicates neoformation of I/S during the ordered stage of illitization. Recent TEM data offers some potential for interpreting reaction mechanisms, but so far the data seem to show that different reactions may occur in similar materials. For example, both Bell (1986) and Klimintidis and Mackinnon (1986) observed an intimate intergrowth of illite and smectite layers within crystallites, whereas Ahn and Peacor (1986) interpreted their data as segregation of illite and smectite layers in diagenetically altered shale. Yau et al. (1987) observed both the segregation of illite packets within a smectitic matrix and the formation of euhedral illite in the Salton Sea geothermal system and attributed both textures to a dissolution-precipitation reaction mechanism. These observations, taken together, demonstrate that generalizations are not yet warranted when describing the illitization reaction in a particular rock type.

Savin (1980) concluded that isotope exchange between water and most minerals is slow at sedimentary temperatures except when reaction between the two phases proceeds. At higher temperatures, some exchange may take place without obvious reactions. Yeh and Savin (1977) demonstrated that the oxygen isotopes in diagenetic I/S were reset progressively as the illitization reaction proceeded and may have reached equilibrium at temperatures over 100 °C. If our data can be applied to natural systems, then the random stage of illitization may be accompanied by incomplete isotopic resetting, whereas the ordered stage may be accompanied by complete isotopic resetting of each illite layer formed. The entire mineral was not equilibrated with the fluids until all layers were illite. It is clear that the interpretation of the isotopic composition of I/S must be done cautiously.

The kinetics of the illitization reaction are important to geologists who try to use the extent of illitization as a thermal-maturation indicator. Hower et al. (1976) and Hoffman and Hower (1979), among others, demonstrated the empirical relationship between burial temperature and the extent of illitization. This relationship has been used by many workers to infer paleotemperatures and diagenetic grade. Other geologists have identified important exceptions to the general relationship between illitization and thermal grade; thus, we know that other variables in addition to temperature must be important to the illitization reaction. Nevertheless, the empirical observations and relationships will continue to be important and useful.

In summary, our ability to interpret mineral, chemical,

isotopic, and textural data from natural samples of I/S is dependent upon our knowledge of the specific characteristics of the reaction process and the effects of several key variables on the reaction. For example, I/S in a sandstone may react differently than I/S in an adjacent shale because of differences in interstitial-fluid composition and volume. But I/S in two sandstones may react differently for the same reasons. The reactivity of I/S found in hydrothermally altered volcanic rocks may differ from that in shales because of differences in starting materials, but temperature, time, and fluid composition may also be different, so it is not possible to assign differences in observed expandabilities to specific variables without a sound empirical and experimental basis.

Conclusions

The reaction of K-exchanged smectite to interstratified I/S proceeded in three stages (random, transition, and ordered) via two reaction mechanisms (transformation and neoformation). In the first (random) stage, randomly interstratified I/S developed by a transformation mechanism that was accompanied by approximately 65% isotopic resetting of the structural oxygen in the illite layers. When the expandability was reduced to approximately 60%, an additional reaction began, which formed ordered I/S. Between 60 and 40% expandability we observed a transition stage during which both random and ordered I/S coexisted. By the time the expandability reached 40%, only ordered I/S remained. The formation of ordered I/S during the ordered stage of the reaction was accompanied by 100% resetting of the isotopes in each illite layer formed, more consistent with a neoformation (dissolution-precipitation) process. Thus, it appears that the illitization reaction in these experiments actually proceeded via two reaction mechanisms.

The rate and nature of the reaction were influenced by the starting material and by the availability of K. Different bentonitic smectites exhibited different reaction rates even though chemically and mineralogically similar. The addition of K to the fluids drove the reaction to more illitic I/S and, at higher temperatures, changed the nature of the reaction by producing more I/S and less chlorite.

All starting materials used in our experiments were bentonitic aluminous smectites. These materials may approximate the composition of altered bentonites observed in nature, but these results should not be applied indiscriminantly to all alteration reactions of smectite to I/S. Further work must be done before the applicability is known because other aluminous smectitic materials may behave differently. In addition, because K was the only interlayer cation present, rates of illitization derived from these studies may not precisely model natural systems. Detailed systematic studies of cation competition must be performed to define the exact effects of K availability in mixed-cation environments on the rate and extent of illitization. Until this information is available, diagenetic models requiring precise information about the illitization reaction must use qualitative and semiquantitative information.

Acknowledgments

We thank L. R. Mahrt, Jr., for preparation of the hydrothermal experimental runs and Kenneth Esposito for the sample preparation and X-ray diffraction analyses. We thank Dennis Eberl and Marc Bodine for constructive reviews of the original manuscript and for many fruitful discussions on the nature of illite/smectite. We also thank Samuel Goldich, who made several helpful suggestions, and Robert C. Reynolds, Jr., Stephen Altaner, and Bruce Velde for their constructive reviews.

References

Ahn, J.H., and Peacor, D.R. (1986) Transmission and analytical electron microscopy of the smectite-to-illite transition. Clays and Clay Minerals, 34, 165–179.

Altaner, S.P., Hower, J., Whitney, G., and Aronson, J.L. (1984) Model for K-bentonite formation: Evidence from zoned K-bentonites in the Disturbed Belt, Montana. Geology, 12, 412–415.

Anjos, S.M.C. (1986) Absence of clay diagenesis in Cretaceous-Tertiary marine shales, Campos Basin, Brazil. Clays and Clay Minerals, 34, 424–434.

Bell, T.E. (1986) Microstructure in mixed-layer illite/smectite and its relationship to the reaction of smectite to illite. Clays and Clay Minerals, 34, 146–154.

Bethke, C.M., and Altaner, S.P. (1986) Layer-by-layer mechanism of smectite illitization and application to a new rate law. Clays and Clay Minerals, 34, 136–145.

Bethke, C.M., Vergo, N., and Altaner, S.P. (1986) Pathways of smectite illitization. Clays and Clay Minerals, 34, 125–135.

Chang, H.K., Mackenzie, F.T., and Schoonmaker, J. (1986) Comparisons between the diagenesis of dioctahedral and trioctahedral smectite, Brazilian offshore basins. Clays and Clay Minerals, 34, 407–423.

Clayton, R.N., and Mayeda, T.K. (1963) The use of bromine pentafluoride in the extraction of oxygen from oxides and silicates for isotopic analysis. Geochimica et Cosmochimica Acta, 27, 43–52.

Eberl, D.D., and Hower, J. (1976) Kinetics of illite formation. Geological Society of America Bulletin, 87, 1326–1330.

Eberl, D.D., Whitney, G., and Khoury, H. (1978) Hydrothermal reactivity of smectite. American Mineralogist, 63, 401–409.

Hoffman, J., and Hower, J. (1979) Clay mineral assemblages as low grade metamorphic geothermometers: Application to the thrust-faulted Disturbed Belt of Montana, U.S.A. In P.A. Scholle and P.R. Schluger, Eds., Aspects of diagenesis. Society of Economic Paleontologists and Mineralogists Special Publication 26, 55–80.

Howard, J.J., and Roy, D.M. (1985) Development of layer charge and kinetics of experimental smectite alteration. Clays and Clay Minerals, 33, 81–88.

Hower, J., Eslinger, E., Hower, M.E., and Perry, E.A. (1976) Mechanism of burial metamorphism of argillaceous sediment: 1. Mineralogical and chemical evidence. Geological Society of America Bulletin, 87, 725–737.

Inoue, A. (1983) Potassium fixation by clay minerals during hydrothermal treatment. Clays and Clay Minerals, 31, 81–91.

Keller, W.D., Reynolds, R.C., and Inoue, A. (1986) Morphology of clay minerals in the smectite-to-illite conversion series by scanning electron microscopy. Clays and Clay Minerals, 34, 187–197.

Klimintidis, R.E., and Mackinnon, I.D.R. (1986) High-resolution imaging of ordered mixed-layer clays. Clays and Clay Minerals, 34, 155–164.

Nadeau, P.H., and Bain, D.C. (1986) Composition of some smectites and diagenetic illitic clays and implications for their origin. Clays and Clay Minerals, 34, 455–464.

Nadeau, P.H., Tait, J.M., McHardy, W.J., and Wilson, M.J. (1984a) Interstratified XRD characteristics of physical mixtures of elementary clay particles. Clay Minerals, 19, 67–76.

Nadeau, P.H., Wilson, M.J., McHardy, W.J., and Tait, J.M. (1984b) Interstratified clays as fundamental particles. Science, 225, 923–925.

——— (1984c) Interparticle diffraction: A new concept for interstratified clays. Clay Minerals, 19, 757–769.

——— (1985a) The conversion of smectite to illite during diagenesis: Evidence from some illitic clays from bentonites and sandstones. Mineralogical Magazine, 49, 393–400.

——— (1985b) Interstratified clays as fundamental particles: A reply. Clays and Clay Minerals, 33, 560.

Pollastro, R.M. (1985) Mineralogical and morphological evidence for the formation of illite at the expense of illite/smectite. Clays and Clay Minerals, 33, 265–274.

Pytte, A.P. (1982) The kinetics of the smectite to illite reaction in contact metamorphic shales. M.S. thesis, Dartmouth College, Hanover, New Hampshire, 78 p.

Reynolds, R.C. (1980) Interstratified clay minerals. In G.W. Brindley and G. Brown, Eds., Crystal structures of clay minerals and their X-ray identification, p. 249–303. Mineralogical Society, London.

Roberson, H.E., and Lahann, R.W. (1981) Smectite to illite conversion rates: Effects of solution chemistry. Clays and Clay Minerals, 29, 129–135.

Savin, S.M. (1980) Oxygen and hydrogen isotope effects in low-temperature mineral-water interactions. In P. Fritz and J.Ch. Fontes, Eds., Handbook of environmental isotope geochemistry, vol. 1, p. 283–328. Elsevier, New York.

Sawhney, B.L., and Reynolds, R.C., Jr. (1985) Interstratified clays as fundamental particles: A discussion. Clays and Clay Minerals, 33, 559.

Środoń, J. (1980) Precise identification of illite/smectite interstratifications by X-ray powder diffraction. Clays and Clay Minerals, 28, 401–411.

——— (1984) X-ray powder diffraction identification of illitic materials. Clays and Clay Minerals, 32, 337–349.

Środoń, J., Morgan, D.J., Eslinger, E.V., Eberl, D.D., and Karlinger, M.R. (1986) Chemistry of illite/smectite and end-member illite. Clays and Clay Minerals, 34, 368–378.

Whitney, G., and Northrop, H.R. (1987) Diagenesis and fluid flow in the San Juan Basin, New Mexico: Regional zonation in the mineralogy and stable isotope composition of clay minerals in sandstone. American Journal of Science, 287, 353–382.

Yau, Y-C., Peacor, D.R., and McDowell, S.D. (1987) Smectite-to-illite reactions in Salton Sea shales: A transmission and analytical electron microscopy study. Journal of Sedimentary Petrology, 57, 335–342.

Yeh, H.W., and Savin, S.M. (1977) The mechanism of burial metamorphism of argillaceous sediments, 3. Oxygen-isotope evidence. Geological Society of America Bulletin, 88, 1321–1330.

Manuscript received March 12, 1987
Manuscript accepted September 23, 1987